

# Disrupted Brain Network in Progressive Mild Cognitive Impairment Measured by Eigenvector Centrality Mapping is Linked to Cognition and Cerebrospinal Fluid Biomarkers

Tiantian Qiu<sup>a,1</sup>, Xiao Luo<sup>a,1</sup>, Zhuqing Shen<sup>a</sup>, Peiyu Huang<sup>a</sup>, Xiaojun Xu<sup>a</sup>, Jiong Zhou<sup>b</sup>,  
Minming Zhang<sup>a,\*</sup> and for the Alzheimer's Disease Neuroimaging Initiative<sup>2</sup>

<sup>a</sup>Department of Radiology, The Second Affiliated Hospital, Zhejiang University School of Medicine, Hangzhou, China

<sup>b</sup>Department of Neurology, The Second Affiliated Hospital, Zhejiang University School of Medicine, Hangzhou, China

Accepted 12 July 2016

**Abstract.** Mild cognitive impairment (MCI) is a heterogeneous condition associated with a high risk of progressing to Alzheimer's disease (AD). Although functional brain network alterations have been observed in progressive MCI (pMCI), the underlying pathological mechanisms of network alterations remain unclear. In the present study, we evaluated neuropsychological, imaging, and cerebrospinal fluid (CSF) data at baseline across a cohort of: 21 pMCI patients, 33 stable MCI (sMCI) patients, and 29 normal controls. Fast eigenvector centrality mapping (fECM) based on resting-state functional MRI (rsfMRI) was used to investigate brain network organization differences among these groups, and we further assessed its relation to cognition and AD-related pathology. Our results demonstrated that pMCI had decreased eigenvector centrality (EC) in left temporal pole and parahippocampal gyrus, and increased EC in left middle frontal gyrus compared to sMCI. In addition, compared to normal controls, patients with pMCI showed decreased EC in right hippocampus and bilateral parahippocampal gyrus, and sMCI had decreased EC in right middle frontal gyrus and superior parietal lobule. Correlation analysis showed that EC in the left temporal pole was related to Wechsler Memory Scale-Revised Logical Memory (WMS-LM) delay score ( $r=0.467$ ,  $p=0.044$ ) and total tau (t-tau) level in CSF ( $r=-0.509$ ,  $p=0.026$ ) in pMCI. Our findings implicate EC changes of different brain network nodes in the prognosis of pMCI and sMCI. Importantly, the association between decreased EC of brain network node and pathological changes may provide a deeper understanding of the underlying pathophysiology of pMCI.

**Keywords:** Alzheimer's disease, brain network organization, cerebrospinal fluid, cognition, mild cognitive impairment, pathophysiology

<sup>1</sup>These authors contributed equally to this work.

<sup>2</sup>Data used in preparation of this article were obtained from the Alzheimer's disease Neuroimaging Initiative (ADNI) database (<http://www.loni.usc.edu>). As such, the investigators within the ADNI contributed to the design and implementation of ADNI and/or provided data but did not participate in analysis or writing of this report. A complete listing of

ADNI investigators can be found at: [http://adni.loni.usc.edu/wp-content/uploads/how\\_to\\_apply/ADNI\\_Acknowledgement\\_List.pdf](http://adni.loni.usc.edu/wp-content/uploads/how_to_apply/ADNI_Acknowledgement_List.pdf)

\*Correspondence to: Minming Zhang, Department of Radiology, The Second Affiliated Hospital, Zhejiang University School of Medicine, No.88 Jiefang Road, Shangcheng District, Hangzhou 310009, China. Tel./Fax: +86 057187315255; E-mail: zhangminming@zju.edu.cn.

## INTRODUCTION

Alzheimer's disease (AD) is the most common type of dementia in the elderly, accompanied by progressive and irreversible cognitive decline. No effective treatment currently exists and this morbidity impacts the afflicted individuals and their families alike due to the accompanying financial and emotional stresses associated with caregiving. Recently, research has focused on improving our understanding of the pre-dementia stage, in the hopes of facilitating early intervention and inhibiting progression. Mild cognitive impairment (MCI) refers to the symptomatic pre-dementia phase of AD [1]. While longitudinal studies have demonstrated that the conversion rate from MCI to AD is approximately 8.3 to 28% [2, 3], more than half of all MCI patients will not progress to dementia over a 10-year follow-up period [4, 5]. Owing to the heterogeneous nature of MCI, a better understanding of the pathophysiological mechanisms of progressive MCI (pMCI) versus stable MCI (sMCI) may facilitate earlier diagnosis and treatment.

Extracellular amyloid- $\beta$  (A $\beta$ ) and intercellular phosphorylated tau (p-tau) protein depositions are recognized as the characteristic pathological alterations in AD, which can be detected at a very early stage [6]. By using  $^{11}\text{C}$ -PIB PET, some studies found that pMCI had increased A $\beta$  deposition in the posterior cingulate, frontal, temporal, and parietal cortices relative to sMCI [7–9]. In cerebrospinal fluid (CSF), decreased A $\beta$  levels and elevated total-tau (t-tau) and p-tau levels were observed in pMCI relative to sMCI, and could also predict conversion from MCI to AD with an accuracy of 70–94% [10, 11].

Recently, resting-state functional magnetic resonance imaging (rsfMRI) has been used to explore brain network functional alterations in patients with pMCI versus sMCI. Based on *a priori* subnetworks, several studies demonstrated that patients with pMCI showed disrupted functional connectivity in the default mode network (DMN) compared with sMCI [12–15]. Using whole-brain network analysis, another study found that the functional connectivity strengths of the left angular gyrus and middle occipital gyrus were significantly lower in pMCI relative to sMCI groups [16]. Although these studies indicate brain network functional disruptions in pMCI, the underlying pathological mechanisms of network disruptions remain unclear. Previous studies have demonstrated a correlation between brain network functional changes and pathological alterations in AD, MCI, and the normal

elderly [17–20], thus we speculate that network alterations in pMCI could be related to pathological abnormalities.

In the present study, we investigated the whole-brain network organization of patients with pMCI and sMCI using fast eigenvector centrality mapping (fECM). This analytical method could detect each brain region serving as a hub, which has greater connectivity with other regions of the brain. The fECM permits the efficient exploration of global organization of the whole-brain network without *a priori* definitions of subnetworks and brain regions [21]. Second, we explored whether changes in brain network organization of pMCI and sMCI patients were related to cognition, and AD-related pathological markers such as amyloid and tau proteins in CSF.

## MATERIAL AND METHODS

### Study design

Data used in the preparation of this article were obtained from the Alzheimer's Disease Neuroimaging Initiative (ADNI) database (<http://adni.loni.usc.edu/>). The primary goal of ADNI has been to test whether serial MRI, positron emission tomography, other biological markers, and clinical and neuropsychological assessments can be combined to measure the progression of MCI and early AD. Participants in ADNI included cognitively normal older individuals, people with early or late MCI, and people with early AD. The follow-up duration of each group is specified in the protocols for ADNI-1, ADNI-2, and ADNI-GO. Subjects originally recruited for ADNI-1 and ADNI-GO had the option to be followed in ADNI-2. The research protocol was approved by each local institutional review board, and written informed consent was obtained from each participant. For up-to-date information, see <http://www.adni-info.org>.

### Subjects

All MCI patients and normal controls were obtained from the ADNI-GO and ADNI-2 database. ADNI criteria for MCI were: 1) subjective memory complaints, either self-reported, reported by a study partner, or reported by a clinician; 2) objective memory loss defined as scoring below an education-adjusted cut-off score on delayed recall of the WMS-R logical memory test; 3) a global Clinical Dementia Rating score of 0.5; 4) a Mini-Mental State

Examination (MMSE) score of equal to, or higher than, 24 out of 30; and 5) general cognitive and functional performance sufficiently preserved such that a diagnosis of dementia could not be made by the site physician at the time of screening [22]. The pMCI was defined as diagnostic status changing from MCI to AD according to the NINCDS-ADRDA criteria [23] within four years. The sMCI was defined as diagnostic status remaining as MCI for a minimum of three years. Demographic, neuropsychological, CSF, and imaging data at baseline of pMCI and sMCI patients were collected. Criteria for normal controls were defined as: a MMSE score of equal to or higher than 24 out of 30; a Clinical Dementia Rating score of 0; and having no report of any cognition complaint. According to the criteria described above, 21 pMCI patients, 38 sMCI patients, and 29 normal controls were included in this study. Five sMCI patients were excluded due to poor imaging data quality, as detailed described in imaging preprocessing (below). Finally, the rest of the subjects (21 pMCI, 33 sMCI, and 29 normal controls) were used for further analysis.

#### *Demographic, neuropsychological, and CSF data acquisition*

Procedures for assessing demographic status, neuropsychological tests, and CSF biomarkers in the ADNI cohort were previously described [22, 24]. In the present study, data are limited to baseline measures. Demographic status was assessed using age, sex, education level, and APOE $\epsilon$ 4 status. The neuropsychological assessments were comprehensive and involved in multiple cognition domains, including: MMSE; Wechsler Memory Scale-Revised Logical Memory II (WMS-LM) immediate and delayed memory; Trails A; semantic verbal fluency (SVF); and the Boston naming test (BNT).

CSF biomarkers included: amyloid-beta 1–42 (A $\beta$ <sub>1–42</sub>), total tau (t-tau), and phosphorylated tau at position 181 (p-tau<sub>181</sub>), which were all measured using the multiplex xMAPLuminex platform (Luminex) with Innogenetics (INNOBIA AlzBio3) immunoassay kit-based reagents. The samples for CSF analyses included 19 out of 21 pMCI patients, 27 out of 33 sMCI patients, and 25 out of 29 normal controls.

#### *Imaging data acquisition*

Both baseline structural and resting-state functional image data were downloaded from the

ADNI database. All subjects were scanned using a 3.0-Tesla Philips MRI scanner. The structural images were acquired using a 3D MPRAGE T1-weighted sequence with the following parameters: repetition time (TR)=2300 ms; echo time (TE)=2.98 ms; inversion time (TI)=900 ms; 170 sagittal slices; within plane FOV = 256×240 mm<sup>2</sup>; voxel size = 1.1×1.1×1.2 mm<sup>3</sup>; flip angle = 9°; bandwidth = 240 Hz/pix. Resting-state functional MRI (rsfMRI) images were obtained using an echo-planar imaging sequence with the following parameters: 140 time points; TR = 3000 ms; TE = 30 ms; number of slices = 48; slice thickness = 3.3 mm; spatial resolution = 3.31×3.31×3.31 mm<sup>3</sup>; flip angle = 80°; and matrix = 64×64.

#### *Imaging preprocessing*

Before image preprocessing, all structural and resting-state functional images were visually inspected. Four sMCI patients (one with an infarct in the left centrum semiovale and three with poor rsfMRI image quality) were excluded from the study. Image data were preprocessed using the Data Processing Assistant for Resting-state fMRI Advanced Edition (DPARSFA, Yan and Zang; <http://rfmri.org/DPARSA>). Firstly, the first 10 image volumes of rsfMRI images were discarded whilst awaiting signal equilibrium and the subject's adaptation to the scanning noise, followed by slice timing and head motion correction (six-parameter rigid body). Imaging data with more than 3.0 mm maximum displacement in any of the x, y, or z directions or 3.0° of any angular motion were excluded (including one sMCI patient). Subsequently, the T1-weighted image was co-registered to the mean rsfMRI image based on rigid-body transformation, and spatially normalized to the Montreal Neurological Institute (MNI) space, then re-sampled into 3×3×3 mm<sup>3</sup> cubic voxels. The rsfMRI images were spatially smoothed with a Gaussian kernel of 6×6×6 mm<sup>3</sup> full width at half maximum. Finally, linear trend adjustment and temporal filtering (0.01 Hz < f < 0.08 Hz) were performed. In order to remove any residual effects of motion and other non-neuronal factors, six head motion parameters, white matter signals, and cerebrospinal fluid signals were regressed out. In addition, the framewise displacement (FD) value was computed for each subject in order to correct for the head motion artifacts.

## ECM

Pre-processed rsfMRI data were further performed with the fast ECM (fECM) tool [25], which yielded a voxel-wise measure of relevance to the functional brain network. The fECM was transformed by the Fisher's  $z$  test. Specially, the human brain is organized as complex networks with small-world properties. Graph theory-based network analysis can be used to investigate the global organization of the whole-brain networks. Eigenvector centrality (EC) is a whole-brain network analytical measure based on graph theory by weighting every nodes based on their degree (both the number and the quality) of connection with the whole brain [26]. Therefore, brain regions with greater EC values mean greater connectedness with the rest of brain and vice versa. The fECM tool is faster and computationally more efficient than traditional ECM calculation methods, because it computes matrix-vector products without having to compute or store the connectivity matrix [25]. Recently, several studies have reported that fECM is an effective method to evaluate whole-brain network alterations by its successful application in AD and Parkinson's disease [21, 27].

### Statistical analysis

Statistical analysis of demographic, neuropsychological, and CSF data was performed using SPSS 21.0 statistical software. Normal distribution was tested using the Kolmogorov-Smirnov test. For continuous variables, we first performed a group-level analysis for pMCI, sMCI, and normal control groups using one-way analysis of variance (ANOVA) and a Kruskal-Wallis test. If group-level test results were significant, *post-hoc* pairwise comparisons were additionally performed (Bonferroni multiple comparison correction in parametric tests, Dunn multiple comparison tests in nonparametric tests). Binary data, such as sex and APOE $\epsilon$ 4, were compared by a chi-square test.

The statistical analysis of fECM was performed using REST software (<http://www.restfmri.net>). ANOVA analysis was performed to identify brain network organization alterations among the three groups with age, gender, education, APOE genotype, and head motion (FD\_value) as covariates. The threshold was set at single voxel  $p < 0.05$  and cluster size  $> 86$  voxels, corresponding to a corrected  $p < 0.05$ , using AlphaSim for multiple comparison corrections (<http://afni.nimh.nih.gov/pub/dist/doc/manual/AlphaSim.pdf>) within the gray matter

mask (excluding the cerebellum due to scanning range). Areas showing significant group effects by ANOVA were used as mask for two-sample  $t$ -test *post-hoc* analyses. The threshold here was set at single voxel  $p < 0.05$  and cluster size  $> 27$  voxels, corresponding to a corrected  $P < 0.05$  using AlphaSim for multiple comparison corrections. Signals from the clusters that showed significant differences between pMCI and sMCI patients were extracted to further test the correlation with cognition and CSF biomarkers using Pearson's correlations.

## RESULTS

### Demographic, neuropsychological, and CSF data

There was no significant difference in age, sex, education level, and the percentage of APOE $\epsilon$ 4 allele between the three groups ( $p > 0.05$ ). The pMCI and sMCI had no significant difference in neuropsychological scores ( $p > 0.05$ ). In CSF biomarkers, pMCI had higher t-tau level than sMCI ( $p = 0.023$ ). In addition, there was no difference in head motion ( $p > 0.05$ ) resulting from the motion correction (Table 1).

### EC differences between the three groups

The direct comparison between pMCI and sMCI revealed that pMCI showed significantly decreased EC in the left temporal pole and the parahippocampal gyrus and increased EC in left middle frontal gyrus. When compared with normal control, pMCI had decreased EC in the right hippocampus and bilateral parahippocampal gyrus, sMCI showed decreased EC in the right middle frontal gyrus and the superior parietal lobule (Fig. 1; Table 2).

### Correlation of EC differences with cognition and CSF biomarkers in pMCI and sMCI

We studied the relationships between EC in left temporal pole, parahippocampal gyrus, and middle frontal gyrus with cognition and CSF biomarkers, given that EC in these regions significantly differed between pMCI and sMCI. In the pMCI group, significant correlations were only found between EC in the left temporal pole with WMS-LM delay score ( $r = 0.467, p = 0.044$ ) and t-tau level ( $r = -0.509, p = 0.026$ ). In the sMCI group, no association between EC alterations with cognition and CSF biomarkers was observed. Across MCI groups, we only found that EC in the left temporal pole was associated with t-tau level ( $r = -0.376, p = 0.009$ ), and EC in left parahippocampal gyrus was related to t-tau level

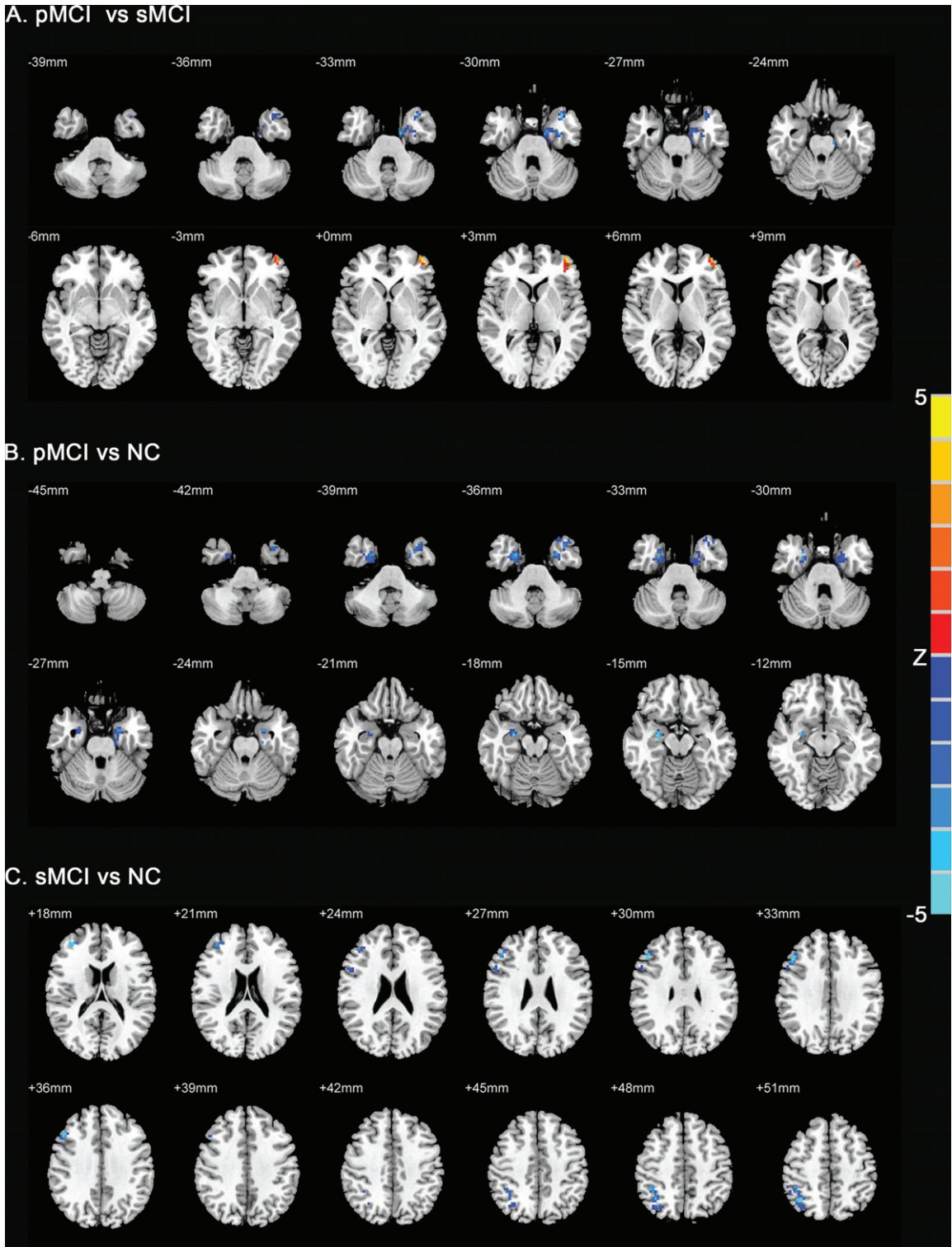


Fig. 1. Statistical parametric map showing the significant differences in EC between three groups: pMCI, sMCI, and normal control (NC). A) EC differences between pMCI and sMCI; B) EC differences between pMCI and NC; and C) EC differences between sMCI and NC. The threshold for display was set to  $p < 0.05$  and cluster size  $> 27$ , corrected by AlphaSim ( $p < 0.05$ ). Areas in blue indicate regions in which the former group had decreased EC compared to the latter group, and areas in red represent the opposite.

Table 1  
Demographic, neuropsychological and CSF data for the three study group

| Variables                                 | pMCI                          | sMCI                      | Normal control | p value |
|---|-------------------------------|---------------------------|----------------|---------|
|   | (n = 21)                      | (n = 33)                  | (n = 29)       |         |
| Age (years)                               | 73.65 ± 4.67                  | 72.45 ± 6.54              | 75.75 ± 5.98   | 0.098   |
| Sex (F:M)                                 | 8 : 13                        | 18 : 15                   | 15 : 14        | 0.476   |
| Education (years)                         | 15.53 ± 2.50                  | 15.85 ± 2.53              | 16.31 ± 2.19   | 0.526   |
| APOEε4 carrier (%)                        | 52.40%                        | 45.50%                    | 37.90%         | 0.593   |
| <i>General mental status</i>              |                               |                           |                |         |
| MMSE                                      | 27.26 ± 1.28 <sup>§§§</sup>   | 27.91 ± 1.51 <sup>#</sup> | 28.83 ± 1.42   | 0.001   |
| <i>Memory function</i>                    |                               |                           |                |         |
| WMS-LM immediate                          | 7.74 ± 4.02 <sup>§§§</sup>    | 9.52 ± 2.49 <sup>##</sup> | 13.97 ± 2.21   | <0.001  |
| WMS-LM delay                              | 5.11 ± 3.09 <sup>§§§</sup>    | 6.91 ± 3.09 <sup>##</sup> | 13.28 ± 2.99   | <0.001  |
| <i>Attention</i>                          |                               |                           |                |         |
| Trails A(s)                               | 45.37 ± 17.91 <sup>§</sup>    | 37.24 ± 15.18             | 33.79 ± 10.40  | 0.027   |
| <i>Language</i>                           |                               |                           |                |         |
| SVF (animal)                              | 16.32 ± 4.81 <sup>§</sup>     | 17.64 ± 4.71              | 20.10 ± 4.75   | 0.021   |
| BNT                                       | 25.89 ± 4.28                  | 28.45 ± 1.69 <sup>#</sup> | 28.48 ± 1.55   | 0.028   |
| <i>CSF biomarkers</i>                     |                               |                           |                |         |
| Aβ <sub>1-42</sub> (pg/ml) <sup>a</sup>   | 150.88 ± 47.34                | 181.73 ± 47.08            | 180.02 ± 47.95 | 0.068   |
| t-tau (pg/ml) <sup>a</sup>                | 122.23 ± 55.82 <sup>§§§</sup> | 83.22 ± 48.31             | 68.97 ± 38.27  | 0.002   |
| p-tau <sub>181</sub> (pg/ml) <sup>a</sup> | 58.71 ± 26.01 <sup>§§</sup>   | 43.28 ± 23.87             | 35.49 ± 18.73  | 0.005   |
| Head Motion                               | 0.30 ± 0.14                   | 0.29 ± 0.18               | 0.31 ± 0.16    | 0.922   |

Values are expressed as mean ± standard deviation or number of participants. MMSE, Mini-Mental State Examination; WMS-LM, Wechsler Memory Scale-Revised Logical Memory II; SVF, semantic verbal fluency; BNT, Boston naming test; CSF: cerebrospinal fluid. <sup>a</sup>71 participants (pMCI = 19, sMCI = 27, NC = 25) have CSF markers. \**p* < 0.05 compared to stable MCI group. §*p* < 0.05 compared to normal control. §§*p* < 0.01 compared to normal control. §§§*p* < 0.001 compared to normal control. #*p* < 0.05 compared to normal control. ##*p* < 0.001 compared to normal control.

Table 2  
EC alterations between the three groups

| Brain regions                   | R/L | Number of voxels | Peak MNI coordinate |     |     | Peak intensity |
|---------------------------------|-----|------------------|---------------------|-----|-----|----------------|
|                                 |     |                  | X                   | Y   | Z   |                |
| <i>pMCI &lt; sMCI</i>           |     |                  |                     |     |     |                |
| Temporal pole                   | L   | 29               | -36                 | 15  | -30 | -3.3811        |
| Parahippocampal gyrus           | L   | 52               | -15                 | -9  | -33 | -3.2094        |
| <i>pMCI &gt; sMCI</i>           |     |                  |                     |     |     |                |
| Middle frontal gyrus            | L   | 42               | -42                 | 54  | 3   | 3.4138         |
| <i>pMCI &lt; normal control</i> |     |                  |                     |     |     |                |
| Hippocampus                     | R   | 30               | 27                  | -9  | -15 | -3.651         |
| Parahippocampal gyrus           | R   | 67               | 24                  | 0   | -36 | -3.2042        |
| Parahippocampal gyrus           | L   | 96               | -21                 | -3  | -27 | -3.0371        |
| <i>sMCI &lt; normal control</i> |     |                  |                     |     |     |                |
| Middle frontal gyrus            | R   | 109              | 48                  | 21  | 36  | -3.4514        |
| Superior parietal lobule        | R   | 88               | 36                  | -60 | 51  | -3.3165        |

(*r* = -0.364, *p* = 0.013). Besides, after adjusting for age, sex, education, and APOE genotype, correlations between EC alterations and t-tau level remained statistically significant (Table 3, Fig. 2).

## DISCUSSION

To our knowledge, this is the first study to explore the correlation of brain network alterations with cognition and CSF biomarkers in pMCI and sMCI patients. The key finding was that EC in the left

temporal pole was associated with memory function and CSF t-tau level in pMCI patients.

We found that patients with pMCI showed decreased EC in the left temporal pole and the parahippocampal gyrus compared to patients with sMCI, and decreased EC in the right hippocampus and bilateral parahippocampal gyrus relative to normal control. This finding is consistent with the “disconnection hypothesis” of AD [28]. Regions with decreased EC are recognized as important nodes of the hippocampal network [29], which plays an

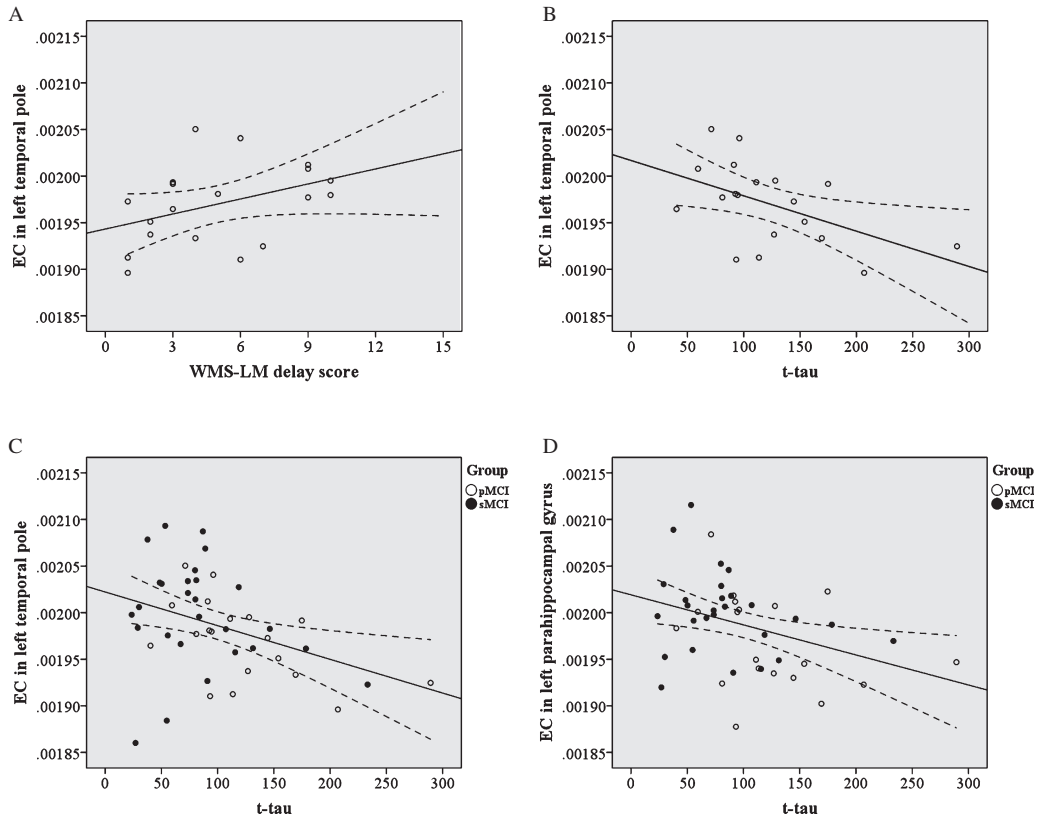


Fig. 2. Scatter plots graphs of relationship between A) EC in left temporal pole and WMS-LM delay score in pMCI group; B) EC in left temporal pole and t-tau level in pMCI group; C) EC in left temporal pole and t-tau level across groups; and D) EC in left parahippocampal gyrus and t-tau level across groups.

Table 3  
Association of altered EC with cognition and CSF biomarkers in pMCI and sMCI groups

|                         | MMSE   | WMS_LM immediate | WMS_LM delay  | SVF    | Trails A | BNT    | Aβ <sub>1-42</sub> | t-tau           | p-tau <sub>181</sub> |
|-------------------------|--------|------------------|---------------|--------|----------|--------|--------------------|-----------------|----------------------|
| <i>pMCI group</i>       |        |                  |               |        |          |        |                    |                 |                      |
| temporal pole_L         | 0.031  | 0.134            | <b>0.467*</b> | 0.054  | 0.181    | 0.075  | 0.287              | <b>-0.509*</b>  | -0.167               |
| parahippocampal gyrus_L | 0.133  | 0.059            | 0.298         | 0.194  | 0.226    | 0.105  | 0.25               | -0.338          | 0.038                |
| middle frontal gyrus_L  | 0.327  | 0.312            | 0.121         | -0.007 | -0.207   | -0.004 | -0.172             | 0.02            | -0.042               |
| <i>sMCI group</i>       |        |                  |               |        |          |        |                    |                 |                      |
| temporal pole_L         | -0.22  | 0.027            | -0.079        | 0.073  | -0.183   | 0.111  | 0.101              | -0.208          | -0.042               |
| parahippocampal gyrus_L | -0.281 | -0.067           | -0.049        | -0.082 | -0.013   | 0.156  | 0.013              | -0.232          | -0.163               |
| middle frontal gyrus_L  | 0.113  | 0.001            | -0.055        | 0.037  | -0.202   | 0.16   | 0.068              | -0.04           | -0.066               |
| <i>PMCI+sMCI groups</i> |        |                  |               |        |          |        |                    |                 |                      |
| temporal pole_L         | -0.039 | 0.108            | 0.153         | 0.094  | -0.098   | 0.106  | 0.233              | <b>-0.376**</b> | -0.156               |
| parahippocampal gyrus_L | 0.006  | 0.076            | 0.188         | 0.096  | -0.005   | 0.108  | 0.21               | <b>-0.364*</b>  | -0.157               |
| middle frontal gyrus_L  | -0.04  | -0.043           | -0.157        | -0.091 | -0.019   | -0.006 | -0.149             | 0.132           | 0.075                |

Data represent correlation coefficients. \* $p < 0.05$ , \*\* $p < 0.01$ . MMSE, Mini-Mental State Examination; WMS-LM, Wechsler Memory Scale-Revised Logical Memory II; SVF, semantic verbal fluency; BNT, Boston naming test.

important role in declarative memory processing and is vulnerable in AD for the convergence of amyloid deposition, brain atrophy, functional disconnection, and hypometabolism [30]. Previous studies have also demonstrated the role of structural and perfusion alterations of hippocampus, parahippocampal gyrus, and temporal pole in the progress of AD. By example,

morphology studies have reported that volumes of hippocampus, parahippocampal gyrus, and temporal pole could predict conversion from MCI to AD [11, 31, 32]. Diffusion-tensor imaging studies revealed that pMCI showed disrupted white matter integrity in the hippocampus and the parahippocampal gyrus [33], as well as in the fornix and the

posterior cingulum (the information transmission pathways from the hippocampal network to the frontal and parietal lobes) relative to sMCI [34, 35]. Several studies also found that hypoperfusion in the medial and inferior temporal cortices could discriminate pMCI patients from sMCI patients [36, 37]. Thus by combining our findings with previously reported results, we propose that the structural and functional alterations in those regions within hippocampal network are related to progression from MCI to AD. In addition, we found increased EC in left middle frontal gyrus in pMCI compared to sMCI. Binnewijzend et al. [21] also found greater EC in AD compared to normal elderly using fECM, which supported our finding. Increased brain network organization in pMCI may indicate a compensation mechanism for the decreased EC in regions within hippocampal network. It should be noted that previous studies on functional alterations of brain network between pMCI and sMCI were mainly within DMN [12–14]. The inconsistencies with our findings may be attributed to different analytical methods in rsfMRI, or the heterogeneity of MCI population.

Furthermore, in the pMCI group, we found that EC in the left temporal pole was positively associated with WMS-LM delay scores, which mainly reflect the episodic memory performance. This result identified the role of temporal pole in memory function. This observation is largely congruent with one animal study that has reported that the temporal pole is related to memory function during an auditory delayed matching-to-sample task [38]. Importantly, supporting evidence was also from AD-related imaging studies. Specially, functional studies have demonstrated that dysfunction of the temporal pole was associated with episodic memory deficits in AD and MCI patients [39, 40]. In addition, structural [41, 42] and metabolic (using proton spectroscopy [43]) neurodegeneration of the temporal pole also significantly correlated with episodic memory impairment in AD and MCI patients. Collectively, memory is the earliest cognitive domain affected by AD, and measures of memory delayed recall are the best neuropsychological predictors of conversion from MCI to AD [44]. However, although there was no statistically significant difference in the WMS-LM delay scores between pMCI and sMCI groups, decreased EC in left temporal pole may reflect the earliest imaging-derived endophenotype underlying memory decline in patients with pMCI. In addition, our result highlighted hub organization of the left

temporal pole which may contribute to memory function in pMCI patients.

In the present study, the pMCI group showed relatively higher t-tau level in CSF than the sMCI group, thus confirming previously reported results [11, 45] and suggesting that increased CSF level of t-tau was associated with an increased risk of progression from MCI to AD [46]. In addition, we further observed the significantly negative correlation between EC in the left temporal pole and CSF t-tau in pMCI group, which may have important implications in the pathogenesis of the pMCI. Particularly, the CSF concentration of t-tau is a sensitive biomarker of incipient neurofibrillary tangles in the brain, which are recognized as the pathological hallmark of AD. Neuropathologic studies in patients with AD also revealed heavy accumulation of neurofibrillary tangles in the temporal pole [47], which may disrupt synaptic plasticity and cause synaptic dysfunction [48]. Moreover, functional connectivity from rsfMRI is thought to reflect the co-varying neuronal signals in spatially distinct brain regions and is recognized as a biomarker of synaptic dysfunction [49]. Thus, we speculated that the association between decreased EC in the left temporal pole and the increased CSF t-tau level indicated that EC could also be a useful imaging marker of AD-related pathological abnormalities in pMCI patients. In addition, previous studies investigating the association of disruption of functional connectivity with CSF biomarkers in AD, MCI patients, and normal elderly also consolidated our findings. Specially, in AD, decreased functional connectivity of dorsal posterior cingulate cortex with retrosplenial cortex in DMN was related to decreased CSF  $A\beta_{1-42}$  level [19]. Li et al. [17] further reported ratio of  $A\beta_{42}/P\text{-tau}_{181p}$  was positively correlated with functional connectivity of left precuneus/cuneus within the DMN in MCI, implicating that functional connectivity within DMN is affected by pathological changes at early stage in AD. In a large number of older adults with normal cognition, Wang et al. [20] revealed decreased CSF  $A\beta_{42}$  and increased CSF ptau<sub>181</sub> were independently associated with reduced functional connectivity in posterior cingulate and medial temporal regions within DMN. Combining our findings and those of previous studies, we propose that functional connectivity changes may reflect AD-related pathological changes of the pMCI patients. However, we did not observe the correlation of EC alterations with CSF  $A\beta_{1-42}$  concentrations in this study. One possible explanation for this is that disrupted EC of pMCI

patients in this study mainly occurred in temporal areas, whereas A $\beta$  plaques may start very early in the neocortex with relatively little in temporal structures [50, 51].

Additionally, we found that sMCI group manifested decreased EC in right middle frontal gyrus and superior parietal lobule relative to normal control. These two regions are important components of right frontal–parietal network, the functions of which include visuospatial integration, coordination, and execution [52]. Previous SPECT studies revealed that sMCI showed cerebral hypoperfusion in frontal and parietal regions relative to normal controls [36, 53]. These observations may suggest that sMCI could disrupt functions of regions mainly within the frontal–parietal network rather than hippocampal network regions, thus leading to the cognitive deficits.

It should be noted that there are inherent limitations associated with this study. First, the sample size of our study was relatively small. Although the ADNI database contains a large amount of data, the number of MCI patients with both resting-state functional MRI data and at least 3 years follow-up were relatively small. Second, due to the relatively short follow-up duration of this study, it should be noted that some MCI patients who were diagnosed as sMCI in the study may later progress to AD. Therefore, larger cohorts and longer-term follow-up of MCI patients will be necessary to validate these findings in future studies. Finally, our study lacked precise proportions of early and late MCI, amnesic and non-amnesic MCI, or single and multi-domain MCI, and the heterogeneity of this population leads to different pathologies. Therefore, future studies that incorporate sufficient numbers of the different types of MCI, that each progress to AD are needed.

### Conclusions

In summary, our findings indicate that there is a different intrinsic network organization between pMCI and sMCI groups. Importantly, the association between decreased EC of brain network node and pathological changes may provide improved understanding of the underlying pathophysiology of pMCI.

### ACKNOWLEDGMENTS

Data collection and sharing for this project were funded by the ADNI (National Institutes of Health [NIH] Grant U01 AG024904). The ADNI is funded by the National Institute on Aging and

the National Institute of Biomedical Imaging and Bioengineering and through generous contributions from the following: Abbott, Alzheimer's Association, Alzheimer's Drug Discovery Foundation, Amorphix Life Sciences, AstraZeneca, Bayer Healthcare, BioClinica, Biogen Idec, Bristol-Myers Squibb, Eisai, Elan Pharmaceuticals, Eli Lilly, F. Hoffmann-La Roche and its affiliated company Genentech, GE Healthcare, Innogenetics, IXICO, Janssen Alzheimer Immunotherapy Research & Development, Johnson & Johnson Pharmaceutical Research & Development, Medpace, Merck, MesoScale Diagnostics, Novartis Pharmaceuticals, Pfizer, Servier, Synarc, and Takeda Pharmaceutical Company. The Canadian Institutes of Health Research is providing funds to support ADNI clinical sites in Canada. Private sector contributions are facilitated by the Foundation for the National Institutes of Health (<http://www.fnih.org>). The grantee organization is the Northern California Institute for Research and Education, and the study is coordinated by the Alzheimer's Disease Cooperative Study at the University of California, San Diego. ADNI data are disseminated by the Laboratory for Neuro Imaging at the University of California, Los Angeles.

This study was also supported by the 12th Five-year Plan for National Science and Technology Supporting Program of China (Grant NO. 2012BAI10B04) and the National Natural Science Foundation of China (Grant Nos.81371519 and 81301190).

Authors' disclosures available online (<http://j-alz.com/manuscript-disclosures/16-0403r2>).

### REFERENCES

- [1] Petersen RC, Smith GE, Waring SC, Ivnik RJ, Tangalos EG, Kokmen E (1999) Mild cognitive impairment: Clinical characterization and outcome. *Arch Neurol* **56**, 303-308.
- [2] Petersen RC, Doody R, Kurz A, Mohs RC, Morris JC, Rabins PV, Ritchie K, Rossor M, Thal L, Winblad B (2001) Current concepts in mild cognitive impairment. *Arch Neurol* **58**, 1985-1992.
- [3] Larrieu S, Letenneur L, Orgogozo JM, Fabrigoule C, Amieva H, Le Carret N, Barberger-Gateau P, Dartigues JF (2002) Incidence and outcome of mild cognitive impairment in a population-based prospective cohort. *Neurology* **59**, 1594-1599.
- [4] Visser PJ, Kester A, Jolles J, Verhey F (2006) Ten-year risk of dementia in subjects with mild cognitive impairment. *Neurology* **67**, 1201-1207.
- [5] Mitchell AJ, Shiri-Feshki M (2009) Rate of progression of mild cognitive impairment to dementia—meta-analysis of 41 robust inception cohort studies. *Acta Psychiatr Scand* **119**, 252-265.

- [6] Scheltens P, Blennow K, Breteler MM, de Strooper B, Frisoni GB, Salloway S, Van der Flier WM (2016) Alzheimer's disease. *Lancet* **388**, 505-517.
- [7] Forsberg A, Engler H, Almkvist O, Blomquist G, Hagman G, Wall A, Ringheim A, Langstrom B, Nordberg A (2008) PET imaging of amyloid deposition in patients with mild cognitive impairment. *Neurobiol Aging* **29**, 1456-1465.
- [8] Waragai M, Okamura N, Furukawa K, Tashiro M, Furumoto S, Funaki Y, Kato M, Iwata R, Yanai K, Kudo Y, Arai H (2009) Comparison study of amyloid PET and voxel-based morphometry analysis in mild cognitive impairment and Alzheimer's disease. *J Neurol Sci* **285**, 100-108.
- [9] Okello A, Koivunen J, Edison P, Archer HA, Turkheimer FE, Nagren K, Bullock R, Walker Z, Kennedy A, Fox NC, Rossor MN, Rinne JO, Brooks DJ (2009) Conversion of amyloid positive and negative MCI to AD over 3 years: An 11C-PIB PET study. *Neurology* **73**, 754-760.
- [10] Shaffer JL, Petrella JR, Sheldon FC, Choudhury KR, Calhoun VD, Coleman RE, Doraiswamy PM (2013) Predicting cognitive decline in subjects at risk for Alzheimer disease by using combined cerebrospinal fluid, MR imaging, and PET biomarkers. *Radiology* **266**, 583-591.
- [11] Eckerstrom C, Olsson E, Bjerke M, Malmgren H, Edman A, Wallin A, Nordlund A (2013) A combination of neuropsychological, neuroimaging, and cerebrospinal fluid markers predicts conversion from mild cognitive impairment to dementia. *J Alzheimers Dis* **36**, 421-431.
- [12] Petrella JR, Sheldon FC, Prince SE, Calhoun VD, Doraiswamy PM (2011) Default mode network connectivity in stable vs progressive mild cognitive impairment. *Neurology* **76**, 511-517.
- [13] Binnewijzend MA, Schoonheim MM, Sanz-Arigita E, Wink AM, van der Flier WM, Tolboom N, Adriaanse SM, Damoiseaux JS, Scheltens P, van Berckel BN, Barkhof F (2012) Resting-state fMRI changes in Alzheimer's disease and mild cognitive impairment. *Neurobiol Aging* **33**, 2018-2028.
- [14] Esposito R, Mosca A, Pieramico V, Cieri F, Cera N, Sensi SL (2013) Characterization of resting state activity in MCI individuals. *PeerJ* **1**, e135.
- [15] Hahn K, Myers N, Prigarin S, Rodenacker K, Kurz A, Forstl H, Zimmer C, Wohlschlagel AM, Sorg C (2013) Selectively and progressively disrupted structural connectivity of functional brain networks in Alzheimer's disease - revealed by a novel framework to analyze edge distributions of networks detecting disruptions with strong statistical evidence. *Neuroimage* **81**, 96-109.
- [16] Li Y, Wang X, Li Y, Sun Y, Sheng C, Li H, Li X, Yu Y, Chen G, Hu X, Jing B, Wang D, Li K, Jessen F, Xia M, Han Y (2016) Abnormal resting-state functional connectivity strength in mild cognitive impairment and its conversion to Alzheimer's disease. *Neural Plast* **2016**, 4680972.
- [17] Li X, Li TQ, Andreasen N, Wiberg MK, Westman E, Wahlund LO (2013) Ratio of Abeta42/P-tau181p in CSF is associated with aberrant default mode network in AD. *Sci Rep* **3**, 1339.
- [18] Malpas CB, Saling MM, Velakoulis D, Desmond P, O'Brien TJ (2016) Differential functional connectivity correlates of cerebrospinal fluid biomarkers in dementia of the Alzheimer's type. *Neurodegener Dis* **16**, 147-1451.
- [19] Celebi O, Uzdogan A, Oguz KK, Has AC, Dolgun A, Cakmakli GY, Akbiyik F, Elibol B, Saka E (2016) Default mode network connectivity is linked to cognitive functioning and CSF A $\beta$ 1-42 levels in Alzheimer's disease. *Arch Gerontol Geriatr* **62**, 125-132.
- [20] Wang L, Brier MR, Snyder AZ, Thomas JB, Fagan AM, Xiong C, Benzinger TL, Holtzman DM, Morris JC, Ances BM (2013) Cerebrospinal fluid Abeta42, phosphorylated Tau181, and resting-state functional connectivity. *JAMA Neurol* **70**, 1242-1248.
- [21] Binnewijzend MA, Adriaanse SM, Van der Flier WM, Teunissen CE, de Munck JC, Stam CJ, Scheltens P, van Berckel BN, Barkhof F, Wink AM (2014) Brain network alterations in Alzheimer's disease measured by eigenvector centrality in fMRI are related to cognition and CSF biomarkers. *Hum Brain Mapp* **35**, 2383-2393.
- [22] Bondi MW, Edmonds EC, Jak AJ, Clark LR, Delano-Wood L, McDonald CR, Nation DA, Libon DJ, Au R, Galasko D, Salmon DP (2014) Neuropsychological criteria for mild cognitive impairment improves diagnostic precision, biomarker associations, and progression rates. *J Alzheimers Dis* **42**, 275-289.
- [23] McKhann G, Drachman D, Folstein M, Katzman R, Price D, Stadlan EM (1984) Clinical diagnosis of Alzheimer's disease: Report of the NINCDS-ADRDA Work Group under the auspices of Department of Health and Human Services Task Force on Alzheimer's Disease. *Neurology* **34**, 939-944.
- [24] Lehallier B, Essioux L, Gayan J, Alexandridis R, Nikolcheva T, Wyss-Coray T, Britschgi M (2015) Combined plasma and cerebrospinal fluid signature for the prediction of midterm progression from mild cognitive impairment to Alzheimer disease. *JAMA Neurol* **73**, 203-212.
- [25] Wink AM, de Munck JC, van der Werf YD, van den Heuvel OA, Barkhof F (2012) Fast eigenvector centrality mapping of voxel-wise connectivity in functional magnetic resonance imaging: Implementation, validation, and interpretation. *Brain Connect* **2**, 265-274.
- [26] Lohmann G, Margulies DS, Horstmann A, Pleger B, Lepsienski J, Goldhahn D, Schloegl H, Stumvoll M, Villringer A, Turner R (2010) Eigenvector centrality mapping for analyzing connectivity patterns in fMRI data of the human brain. *PLoS One* **5**, e10232.
- [27] Lou Y, Huang P, Li D, Cen Z, Wang B, Gao J, Xuan M, Yu H, Zhang M, Luo W (2015) Altered brain network centrality in depressed Parkinson's disease patients. *Mov Disord* **30**, 1777-1784.
- [28] Vallet GT, Hudon C, Simard M, Versace R (2013) The disconnection syndrome in the Alzheimer's disease: The cross-modal priming example. *Cortex* **49**, 2402-2415.
- [29] Trachtenberg AJ, Filippini N, Ebmeier KP, Smith SM, Karpe F, Mackay CE (2012) The effects of APOE on the functional architecture of the resting brain. *Neuroimage* **59**, 565-572.
- [30] Sanchez MM, Moghadam S, Naik P, Martin KJ, Salehi A (2011) Hippocampal network alterations in Alzheimer's disease and Down syndrome: From structure to therapy. *J Alzheimers Dis* **26**(Suppl 3), 29-47.
- [31] Desikan RS, Fischl B, Cabral HJ, Kemper TL, Guttman CR, Blacker D, Hyman BT, Albert MS, Killiany RJ (2008) MRI measures of temporoparietal regions show differential rates of atrophy during prodromal AD. *Neurology* **71**, 819-825.
- [32] Eskildsen SF, Coupe P, Fonov VS, Pruessner JC, Collins DL (2015) Structural imaging biomarkers of Alzheimer's disease: Predicting disease progression. *Neurobiol Aging* **36**(Suppl 1), S23-S31.
- [33] Solodkin A, Chen EE, Van Hoesen GW, Heimer L, Shereen A, Kruggel F, Mastrianni J (2013) *In vivo* parahippocampal

- white matter pathology as a biomarker of disease progression to Alzheimer's disease. *J Comp Neurol* **521**, 4300-4317.
- [34] Mielke MM, Okonkwo OC, Oishi K, Mori S, Tighe S, Miller MI, Ceritoglu C, Brown T, Albert M, Lyketsos CG (2012) Fornix integrity and hippocampal volume predict memory decline and progression to Alzheimer's disease. *Alzheimers Dement* **8**, 105-113.
- [35] van Bruggen T, Stieltjes B, Thomann PA, Parzer P, Meinzer HP, Fritzsche KH (2012) Do Alzheimer-specific microstructural changes in mild cognitive impairment predict conversion? *Psychiatry Res* **203**, 184-193.
- [36] Hirao K, Ohnishi T, Hirata Y, Yamashita F, Mori T, Moriguchi Y, Matsuda H, Nemoto K, Imabayashi E, Yamada M, Iwamoto T, Arima K, Asada T (2005) The prediction of rapid conversion to Alzheimer's disease in mild cognitive impairment using regional cerebral blood flow SPECT. *Neuroimage* **28**, 1014-1021.
- [37] Park KW, Yoon HJ, Kang DY, Kim BC, Kim S, Kim JW (2012) Regional cerebral blood flow differences in patients with mild cognitive impairment between those who did and did not develop Alzheimer's disease. *Psychiatry Res* **203**, 201-206.
- [38] Bigelow J, Ng CW, Poremba A (2016) Local field potential correlates of auditory working memory in primate dorsal temporal pole. *Brain Res* **1640**(Pt B), 299-313.
- [39] Xie C, Bai F, Yu H, Shi Y, Yuan Y, Chen G, Li W, Chen G, Zhang Z, Li SJ (2012) Abnormal insula functional network is associated with episodic memory decline in amnesic mild cognitive impairment. *Neuroimage* **63**, 320-327.
- [40] Gour N, Ranjeva JP, Ceccaldi M, Confort-Gouny S, Barbeau E, Soulier E, Guye M, Didic M, Felician O (2011) Basal functional connectivity within the anterior temporal network is associated with performance on declarative memory tasks. *Neuroimage* **58**, 687-697.
- [41] Tomadesso C, Perrotin A, Mutlu J, Mezenge F, Landeau B, Egret S, de la Sayette V, Jonin PY, Eustache F, Desgranges B, Chetelat G (2015) Brain structural, functional, and cognitive correlates of recent versus remote autobiographical memories in amnesic mild cognitive impairment. *Neuroimage Clin* **8**, 473-482.
- [42] Wolk DA, Dickerson BC (2011) Fractionating verbal episodic memory in Alzheimer's disease. *Neuroimage* **54**, 1530-1539.
- [43] Rami L, Gomez-Anson B, Bosch B, Sanchez-Valle R, Monte GC, Villar A, Molinuevo JL (2007) Cortical brain metabolism as measured by proton spectroscopy is related to memory performance in patients with amnesic mild cognitive impairment and Alzheimer's disease. *Dement Geriatr Cogn Disord* **24**, 274-279.
- [44] Gainotti G, Quaranta D, Vita MG, Marra C (2014) Neuropsychological predictors of conversion from mild cognitive impairment to Alzheimer's disease. *J Alzheimers Dis* **38**, 481-495.
- [45] Heister D, Brewer JB, Magda S, Blennow K, McEvoy LK, Alzheimer's Disease Neuroimaging I (2011) Predicting MCI outcome with clinically available MRI and CSF biomarkers. *Neurology* **77**, 1619-1628.
- [46] Li JQ, Tan L, Wang HF, Tan MS, Tan L, Xu W, Zhao QF, Wang J, Jiang T, Yu JT (2016) Risk factors for predicting progression from mild cognitive impairment to Alzheimer's disease: A systematic review and meta-analysis of cohort studies. *J Neurol Neurosurg Psychiatry* **87**, 476-484.
- [47] Arnold SE, Hyman BT, Van Hoesen GW (1994) Neuropathologic changes of the temporal pole in Alzheimer's disease and Pick's disease. *Arch Neurol* **51**, 145-150.
- [48] Meier S, Bell M, Lyons DN, Rodriguez-Rivera J, Ingram A, Fontaine SN, Mechas E, Chen J, Wolozin B, LeVine H, 3rd, Zhu H, Abisambra JF (2016) Pathological tau promotes neuronal damage by impairing ribosomal function and decreasing protein synthesis. *J Neurosci* **36**, 1001-1007.
- [49] Maestu F, Pena JM, Garces P, Gonzalez S, Bajo R, Bagic A, Cuesta P, Funke M, Makela JP, Menasalvas E, Nakamura A, Parkkonen L, Lopez ME, Del Pozo F, Sudre G, Zamrini E, Pekkonen E, Henson RN, Becker JT (2015) A multicenter study of the early detection of synaptic dysfunction in Mild Cognitive Impairment using magnetoencephalography-derived functional connectivity. *Neuroimage Clin* **9**, 103-109.
- [50] Kempainen NM, Aalto S, Wilson IA, Nagren K, Helin S, Bruck A, Oikonen V, Kailajarvi M, Scheinin M, Viitanen M, Parkkola R, Rinne JO (2007) PET amyloid ligand [11C]PIB uptake is increased in mild cognitive impairment. *Neurology* **68**, 1603-1606.
- [51] Rowe CC, Ng S, Ackermann U, Gong SJ, Pike K, Savage G, Cowie TF, Dickinson KL, Maruff P, Darby D, Smith C, Woodward M, Merory J, Tochon-Danguy H, O'Keefe G, Klunk WE, Mathis CA, Price JC, Masters CL, Villmagne VL (2007) Imaging beta-amyloid burden in aging and dementia. *Neurology* **68**, 1718-1725.
- [52] Laird AR, Fox PM, Eickhoff SB, Turner JA, Ray KL, McKay DR, Glahn DC, Beckmann CF, Smith SM, Fox PT (2011) Behavioral interpretations of intrinsic connectivity networks. *J Cogn Neurosci* **23**, 4022-4037.
- [53] Huang C, Eidelberg D, Habeck C, Moeller J, Svensson L, Tarabula T, Julin P (2007) Imaging markers of mild cognitive impairment: Multivariate analysis of CBF SPECT. *Neurobiol Aging* **28**, 1062-1069.